The Invention Relates to the Design of Noise Reflector Hood Based on Reflective Energy Accumulation Technology

Yaxiong Gu[1], Sai Wu[2, a]

1School of Southwest Petroleum University, Chengdu, 610000, China

2School of Southwest Petroleum University, Chengdu, 610000, China

[a]357088071@qq.com

Abstract

In this paper, after investigating the domestic and foreign literatures on noise power generation technology, it is found that due to various constraints, the efficiency of the noise power generation device designed by the researchers is very low in collecting the noise energy in the environment. In order to improve the efficiency of energy collection, a kind of noise reflector which can gather noise energy is designed. The main research contents of this paper include: According to the acoustic focusing theory and Kirchhoff formula, the theoretical solution of axial reflection sound field in time domain is solved. Then, DR algorithm is introduced into the Kirchhoff formula in convolution form to obtain the three-dimensional numerical solution of the reflected sound field, which provides a theoretical basis for analyzing the acoustic focusing effect of the reflection cover. Finally, the influence of the change of "deep focal ratio" of the parabolic reflector on the acoustic focusing effect is analyzed, and the structure of the reflector is designed.

Keywords

Noise power generation; Acoustic focusing; DR algorithm; Deep coke rate.

1. Introduction

On the basis of reading the related research data of noise power generation technology at home and abroad, a design scheme of noise reflection hood based on reflective energy accumulation technology is proposed. The noise reflector can gather the noise energy in the environment and improve the energy collection efficiency. Firstly, the methods of acoustic focusing are summarized, and the geometric surface reflection method is chosen as the research method in this paper. Then, the one-dimensional theoretical solution of the sound field theory is derived, and the DR algorithm is introduced into the Kirchhoff formula in the convolution form, and the three-dimensional numerical solution of the reflected sound field is obtained, which provides theoretical basis for the subsequent research. Then the three-dimensional numerical solutions of the reflection sound field of the ellipsoid reflector and the parabolic reflector are solved respectively, and the numerical solutions based on the DR method and the standard theoretical solutions are compared and analyzed. Then the acoustic focusing effect of the rotating ellipsoid and the rotating parabolic reflector is compared and analyzed by using MATLAB software. Finally, the optimal deep focal ratio of the parabolic reflector is calculated and the structure of the reflector is designed.

2. Fundamental Theory of Acoustic Focusing

Acoustic focusing is the key technology to achieve acoustic energy convergence. Its main characteristics are easy to implement and good stability, and it has been widely used in real life.

Therefore, the basic theory of acoustic focusing will be studied in this chapter, which will provide theoretical basis for the subsequent performance analysis of noise generation devices.

2.1. Reflection Energy Accumulation Technology

2.1.1 Overview of reflector hood

Reflector is a common acoustic focusing device that has been in use for a long time. This kind of acoustic focusing mode has the advantages of good directivity, good stability and so on, and it is widely used in the fields of national defense, military industry, agriculture, aerospace, daily household appliances and so on.

The principle of using a reflector to achieve acoustic focusing is that the curved reflector with special geometric properties (for example, a rotating paraboloid, an ellipsoid, etc.) makes the acoustic wave change its propagation direction after reflection in the process of propagation and focus on a specified area. Reflector hood is an important tool to realize acoustic focusing, which is of great significance in the study of acoustic focusing effect and acoustic propagation. Compared with other acoustic focusing methods (for example, array focusing method and acoustic lens method), the focusing system composed of a reflector is more controllable and efficient, so the related research field is in urgent need of a reflector with high performance. In order to meet the increasing requirements, it is necessary to improve the focusing sound intensity and efficiency of the reflector.

2.1.2 The method of focusing sound waves

The basic principle of acoustic focusing is to emit sound waves in a set direction. After reflection or transmission, a high energy focused area is formed in a certain space, which improves the propagation distance and intensity of sound waves in the specified direction. At present, the methods of acoustic focusing mainly include: acoustic lens focusing method[1], ultrasonic demodulation acoustic directional method, multi-unit coherent array method, electronic phased array focusing method and geometric surface reflection method.

Common geometric surface focusing methods include rotating paraboloid, concave sphere, conic surface and so on. Geometric surface reflection method has the advantages of good directivity, good focusing effect and wide application range, which is suitable for focusing and bunching of medium and low frequency acoustic waves. In general, the frequency of noise in the application environment in this paper is about 550Hz, which belongs to medium frequency sound wave. Aiming at the application environment of this paper, in order to obtain higher focused acoustic energy, the geometric surface reflection method is used to realize the noise acoustic convergence.

2.2. Numerical Solution Based on DR Method

Using numerical methods to solve the reflected sound field, it is necessary to introduce the DR method into the Kirchhoff acoustic diffraction formula in the form of time-domain convolution [2], and then discretize the integral. The time domain convolution Kirchhoff acoustic diffraction formula can be expressed as

$$p(r,t)=\frac{1}{4\pi}\iint_S\left\{p(r_0,t)*\frac{\partial g(r|r_0,t)}{\partial n_0}-g(r|r_0,t)*\frac{\partial p(r_0,t)}{\partial n_0}\right\}dS \tag{1}$$

Where, "*" is the convolution, $p(r_0, t)$is the sound pressure distribution on $S(r_0)$of the reflector cover surface, g$(r|r_0, t)$is Green's function of acoustic space.

$$\begin{cases} p(r_0,t)=A(r_0)p_0(t)*\delta[t-t_d(r_0)] \\ g(r|r_0,t)=g(|r-r_0|,t)=\dfrac{\delta(t-|r-r_0|/c_0)}{|r-r_0|} \\ G(r|r_0,\omega)=G(|r-r_0|,\omega)=\dfrac{\exp(-jk|r-r_0|)}{|r-r_0|} \end{cases} \tag{2}$$

In the formula, $A(r_0)$ and $t_d(r_0)$ are the sound pressure amplitude distribution and time delay of the secondary source respectively, and $p_0(t)$ is the sound source function. G is Green's function in the time domain and G is Green's function in the frequency domain.

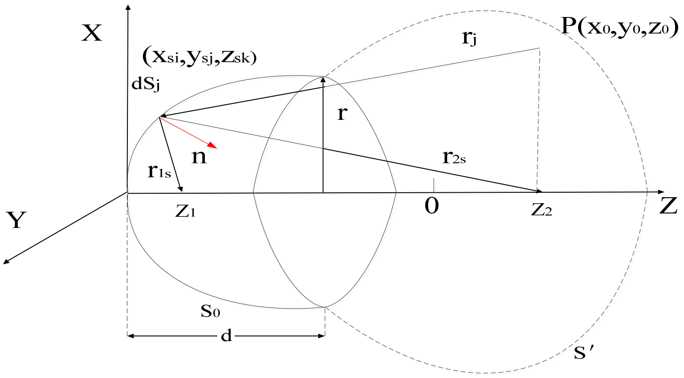

Figure 1. Acoustic diffractometry of a reflectance cumulative system with a rotating surface

In Figure 1, S0 is the surface of the reflector, d is the depth of the reflector, S' is the imaginary infinite half of the sphere, the closed surface is composed of S0 and S', Z_1 is the focus of the reflector, r_{1S} is the distance from a point S_j to Z_1 on the reflector, n is the inner normal of S_j, and r_j is the distance from point p to S_j. The Green's function of the secondary wave source from S0 is

$$g(r|r_0,t)=g(|r-r_0|,t)-g(|r-r_0-2d\cdot n|,t) \tag{3}$$

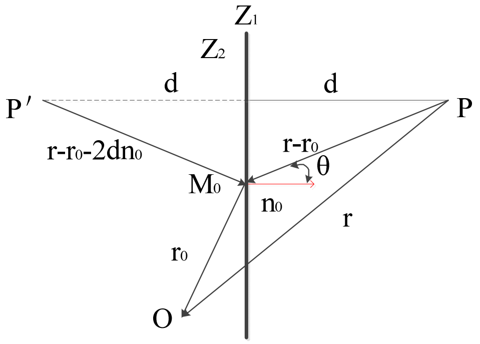

Figure 2. Diagram of Green's function calculation of a secondary radiation source on the surface of a reflector

In Figure 2, 2d is the distance between point p and mirror point P', O is the reference point, M0 is the secondary radiation source on the reflector cover surface, and n0 has a vertical relationship with the internal normal direction of point M0. Z is the acoustic impedance.

$$\begin{cases} g(r|r_0,t)=0 \\ \dfrac{\partial g(r|r_0,t)}{\partial n} = IFT\left\{\dfrac{\partial G(r|r_0,\omega)}{\partial n}\right\} = \dfrac{2}{c_0}\dfrac{\partial g(r|r_0,t)}{\partial t}\cdot\cos(n_0,r-r_0) \end{cases} \tag{4}$$

Type, IFT for the inverse Fourier transform, $\cos(n_0, r-r_0) = (r-r_0)\cdot e_n / |r-r_0|$ for $r-r_0$ Angle cosine with n_0, after finishing can be simplified

$$\begin{cases} p(r,t)=\rho_0\cdot\dfrac{\partial\Phi}{\partial t} * f(t) \\ \Phi = \dfrac{1}{2\pi}\iint_S \cos(n_0,r-r_0)\cdot\dfrac{u_0}{|r-r_0|}\cdot A(r_0)\cdot\delta[t-T_d(r_0)]\cdot dS \end{cases} \tag{5}$$

Equation (5) uses the approximate relation of plane waves $p_0(t) = \rho_0 c_0 u_0 f(t)$ $T_d(r_0)$ is the total delay time, $T_d(r_0) = t_d(r_0) + |r-r_0|/c_0$. According to Equation (5), if Φ is regarded as the displacement potential function, then the solution of the linear wave equation is $p(r,t)$. In the reflector system, given the parameter equations of the reflector hood (ellipsoid, paraboloid, etc.), $\cos(n_0, r-r_0)$, $A(r_0)$ and $T_d(r_0)$ can be calculated, and finally the specific expression of Φ can be calculated.

2.2.1 DR method

In the 1990s, Piwakowski and Delannoy et al [3-4] proposed the DR method (Discrete Representation method). The basic idea is to use the time window function and convolution to obtain the average impact response function in Δt, and then take spatial sampling to obtain the discrete average impact response function. If the sampling rate is high enough, it will be closer to. By means of the discrete average calculation, the complex integral operation of the formula (3) becomes a simple numerical operation.

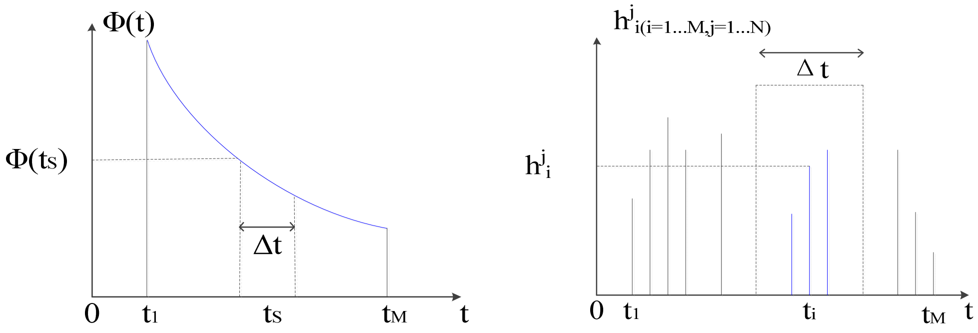

Figure 3. Discrete average of shock response function

In Figure 3, T_1 =min ({T_i,│ I =1... M}), T_m = Max ({T_i,│ I =1... M}) is the latest time. Since it contains the delay time T_D (R_0), {T_i,│ I =1... M} size order is independent of the specific position of the reflector cover surface. DR method is divided into the following two steps:

(1) Calculate the time average impulse response function

In the process of integration, the delta function has the characteristic of filtering, which can be obtained by using the convolution of a delta t width time window function and impulse response function

$$\overline{\Phi}(t)=\frac{1}{\Delta t}\iint_S \frac{1}{2\pi}\cos(n_0,r-r_0)\cdot\frac{u_0}{R}\cdot A(z_S)\cdot\Pi\left[\frac{t-T_d(z_S)}{\Delta t}\right]\cdot dS \tag{6}$$

In order to avoid spectral aliasing, Nequist sampling law is used to value the time step, then Δt≤0.5/f_max.

(2) Discrete $\overline{\Phi}(t)$

$$\overline{\Phi}_d(t)=\frac{1}{\Delta t}\sum_{j=1}^{N}\frac{u_0}{2\pi R_j}\cos(n_0,r-r_0)\cdot A(z_S)\cdot\Pi\left[\frac{t-T_d(z_S)}{\Delta t}\right]\cdot\Delta S_j \tag{7}$$

In the reflecting accumulator system, ΔS_j is the area of the element on the surface of the reflector cover, $S=\sum_{j=1}^{N}\Delta S_j$

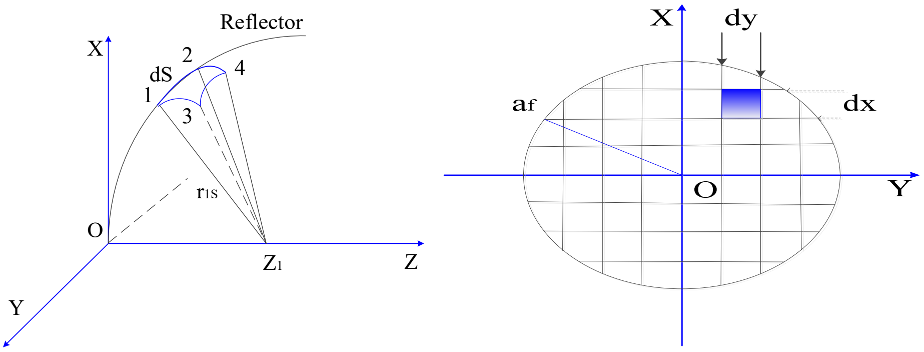

Figure 4. The microelement area on the surface of the reflector is spatially discrete from the outlet surface

As shown in Figure 4, the space element area ΔS_j is

$$\begin{cases}\Delta S_j=\frac{1}{2}(l_{12}\cdot l_{13}+l_{42}\cdot l_{43})\\ l_{12}=\sqrt{\Delta x^2+az_1^2},l_{13}=\sqrt{\Delta x^2+az_4^2}\\ l_{42}=\sqrt{\Delta y^2+az_2^2},l_{43}=\sqrt{\Delta y^2+az_3^2}\end{cases} \tag{8}$$

Where, $az_i(i=1\ldots4)$ is the projection length of each edge l of ΔS_j in XOY plane, Δx and Δy are space steps.

1. For a parabolic reflector, the equation of parabola can be obtained

$$\begin{cases}az_1=az_3=\frac{1}{4F}\left[(x_i+\Delta x_i)^2-x_i^2\right]\\ az_2=az_4=\frac{1}{4F}\left[(y_i+\Delta y_i)^2-y_i^2\right]\end{cases} \tag{9}$$

The a and b are the long and short half axes of the ellipsoid respectively. This paper defined

$$h_i^j = \frac{u_0}{2\pi R_j}\cos(n_0, r - r_0)\cdot A(z_S)\cdot \Pi\left[\frac{t - T_d(z_S)}{\Delta t}\right]\cdot \Delta S_j \tag{10}$$

h_i^j is the amplitude of the impact response function at S_j at the time of t_i, which can be obtained $\overline{\Phi}_d(t_S)$by the time window function Π

$$\overline{\Phi}_d(t_S) = \frac{1}{\Delta t}\sum_{j \Rightarrow (t_i > t_S - \Delta t/2)}^{j \Rightarrow (t_i < t_S - \Delta t/2)} h_i^j \tag{11}$$

Where, "$\Rightarrow$" represents the value of j within this range. According to Equation (14), if the time and space step is small enough, the average discrete value $\overline{\Phi}_d(t_S)$ will be closer to the theoretical value $\Phi_d(t_S)$, then.

$$\lim_{\Delta S \to 0} \overline{\Phi}_d(t_S) = \Phi(t_S) \tag{12}$$

2.3. Chapter Summary

In this chapter, the methods of acoustic focusing are firstly analyzed: acoustic lens focusing method, ultrasonic demodulation acoustic directional method, multi-element coherent array method, electronic phased array focusing method and geometric surface reflection method. According to the actual situation, the geometric surface reflection method is chosen to achieve acoustic convergence. Then, based on the theory of focusing sound field and combining with specific boundary conditions (ellipsoid or paraboloid), the time-domain theoretical solution of the axis of sound wave reflected by a rotating paraboloid is derived. Finally, DR algorithm is introduced into Kirchhoff formula in convolution form to solve the three-dimensional numerical solution of the reflected sound field, which lays a foundation for solving the numerical solution of the reflected sound field in Chapter 3.

3. Numerical solution of reflection sound field and design of reflector hood structure

In chapter 2, the theoretical problem of reflection sound field calculation is studied. The one-dimensional theoretical solution and the three-dimensional numerical solution based on the DR method are obtained by using the Kirchhoff acoustic diffraction formula. In this chapter, the results of ellipsoid reflection focusing and paraboloid reflection focusing are solved numerically respectively, and the optimal deep focal ratio of the paraboloid reflector is calculated, which provides the basis for the structural design of the reflector.

3.1. The Result of The Reflected Sound Field

For the reflection energy accumulation system, after the impulse response function is obtained, the time partial derivative of the impulse response function is obtained. Finally, the solution of the sound field can be obtained by convolving with the pulse waveform of the sound source.

In the reflected energy accumulation system, the propagation medium is air, and the impact pulse waveform with the pressure decreasing exponentially is taken as the input sound wave, then

$$f(t) = A \cdot \exp\left[-\frac{(\omega_0 t)^2}{\Gamma}\right] \cdot \sin(\omega_0 t) \tag{13}$$

3.1.1 An ellipsoid reflector reflects the focus

The 3D acoustic field can also be calculated using DR algorithm. Figure 5 shows the 3D distribution of the acoustic focus of the ellipsoid reflector.

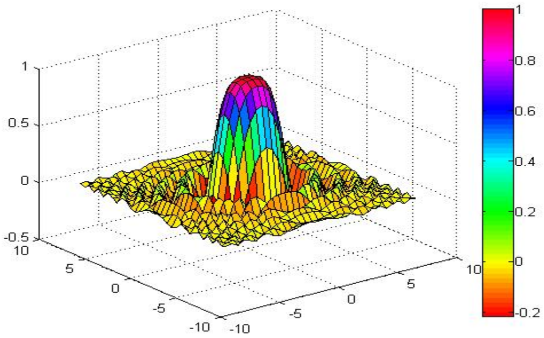

Figure 5. Sonic focusing effect of ellipsoid reflector

As can be seen from Figure 5, the sound waves emitted by the sound source converge to the focal point after being reflected by the reflector, so the ellipsoid reflector has a certain clustering effect on the sound waves. However, the focal spot of the sound source converged by the ellipsoid reflector is large and the directivity is poor.

3.1.2 A parabolic mask reflects the focus

DR algorithm was used to calculate the three-dimensional focusing sound field of the paraboloid reflector. Figure 6 shows the three-dimensional distribution of the acoustic focusing of the paraboloid reflector.

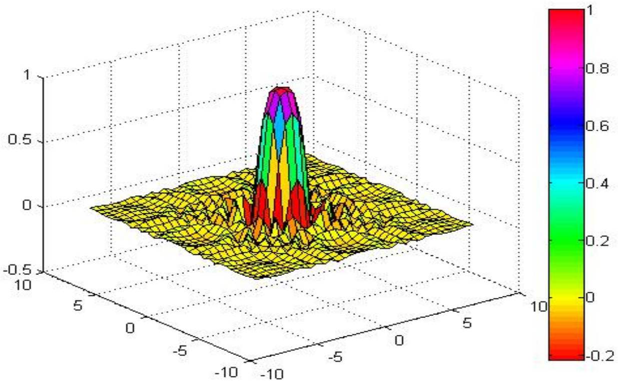

Figure 6. The parabolic mask focuses the sound waves

As shown in figure 6, the sound waves emitted by the sound source are reflected by the parabolic mask and converge to the focal point. Therefore, the parabolic reflector has obvious bunching effect on the acoustic wave, good directivity, sharp beam, less divergent sound lines, and good convergence effect.

3.2. Optimal Deep Focal Ratio of A Parabolic Reflector

3.2.1 The peak power density of the reflected sound field

The peak power density at the observation point is an important index to evaluate the performance of sound source under experimental application conditions. The relationship between peak power density and sound pressure can be expressed as

$$I_p = P_{\max}^2 / 2\rho_0 c_0 \tag{14}$$

According to the one-dimensional theoretical solution, for different deep focal ratios, the variation curve of peak power density along the axis of the reflector housing is obtained through calculation, as shown in Figure 7.

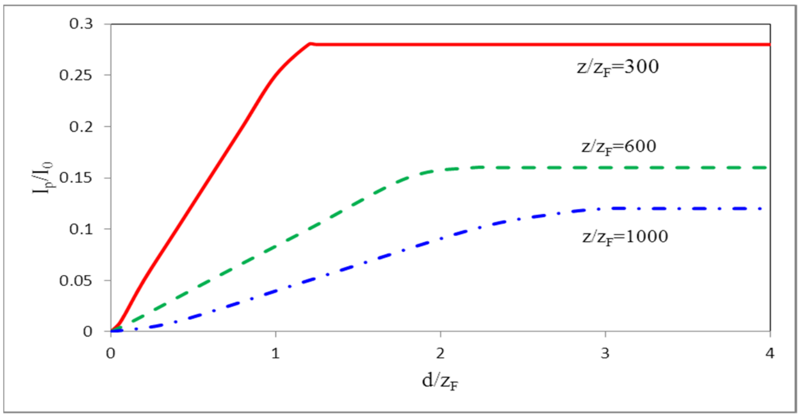

Figure 7. The curve of the density of sound waves at different distances as a function of the deep focal ratio

As can be seen from Figure 7, when the deep focal ratio of the paraboloid increases to a certain value, the peak power density tends to be stable. For example, at $z/z_F = 1000$, the peak power density stops increasing after the deep focal ratio increases to 3. Therefore, the volume requirement of the system and the focus intensity of the reflected wave should be considered to design the parameters of the paraboloid. Therefore, this paper gives some different focal lengths as geometric parameters of the paraboloid, and calculates the value of the limit "deep focal ratio", as shown in Figure 8.

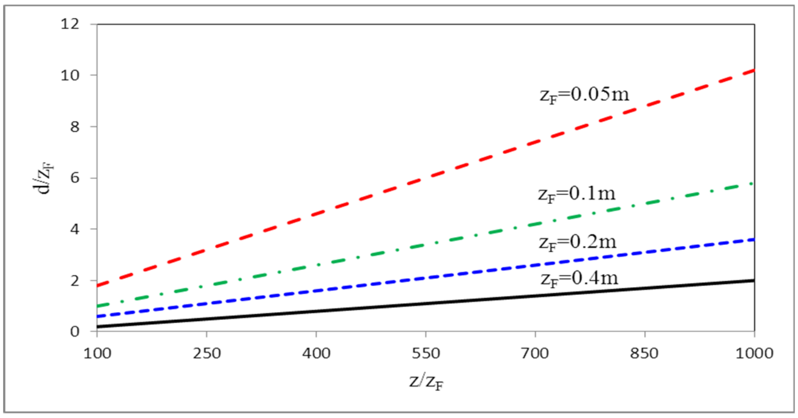

Figure 8. Limit deep focal ratio curves at different distances

As can be seen from Figure 8, the limiting deep focal ratio increases with the increase of propagation distance. For example, when the focal length of a parabolic reflector is 0.1m and its depth increases to 0.34m, the peak power density of the sound source located at the axial distance z=55m at the focal point of the reflector stops increasing. When the acoustic source is located at the axial distance z=100m, the depth is 0.58m. As the focal length of the paraboloid increases, the slope of the line decreases. And under the same propagation distance, the larger the focal length of the reflector, the smaller the limit value of the deep focal ratio.

3.2.2 Analysis of the optimal deep focal ratio

The focal length and depth of the paraboloid can be changed freely while the diameter of the paraboloid is unchanged. In order to maximize the pressure amplitude of the reflected wave at the focal point of the reflector cover, an optimal deep focal ratio parameter was calculated, as shown in Figure 9. In the figure, F_p is the sound pressure amplification ratio of the paraboloid, and F_{pmax} is the peak sound pressure amplification ratio.

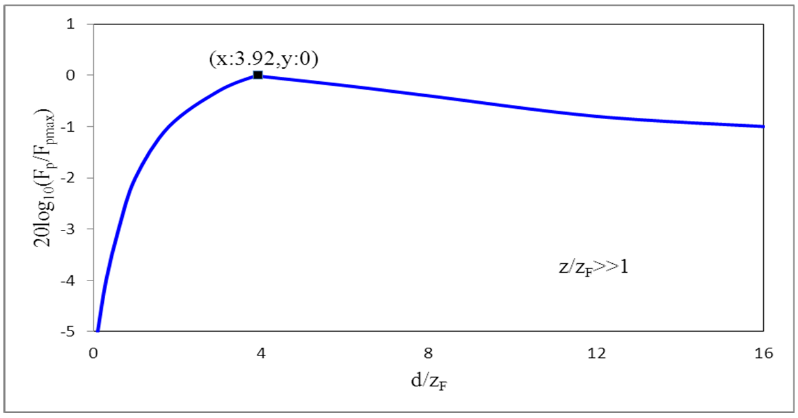

Figure 9. When the diameter of the reflector is fixed, the far-field sound pressure ratio curve is obtained

When the diameter of the parabolic reflector is constant, there must be an optimal deep focal ratio in the far field, $d/z_F = 3.92$, which can make the sound pressure of the reflected wave reach the maximum. In this paper, the deep focus ratio $d/z_F = 4$, which is very close to the calculated value and meets the requirements of the parameter selection of the deep focus ratio of the reflector housing.

3.3. Structure Design of Reflector Hood

From the analysis of the reflector above, it can be seen that the parabolic reflector is better than the ellipsoid in focusing the sound wave, so the parabolic reflector is chosen for the noise aggregation reflector in this paper. When the aperture of the parabolic reflector is 0.4m and the optimal deep focal ratio $d/z_F = 4$, then the focal length $z_F = 5.0\text{cm}$, the maximum sound pressure of the reflected wave can be achieved. Therefore, the structural parameters of the parabolic reflector are selected as follows: depth $d = 0.2\text{m}$, focal length $z_F = 5.0\text{cm}$, and aperture is 0.4m, and good acoustic focusing effect is obtained.

4. Summary

The results of ellipsoid and paraboloid focusing show that the numerical results based on DR method agree well with the theoretical results. Then the sound focusing effect of the rotating ellipsoid and the rotating paraboloid reflector is compared and analyzed by using Matlab software. The simulation results show that the rotating paraboloid reflector is better than the ellipsoid in focusing sound waves. Finally, the optimal deep focal ratio of the parabolic reflector is calculated. When the aperture of the parabolic reflector is constant, there must be an optimal deep focal ratio $d/z_F = 3.92$ in the far field, which can make the sound pressure of the reflected wave reach the maximum value. Based on this, the structure design of the reflector is carried out.

References

[1] Zhang Liqiang, Wu Jianchao, Jiang Chunxu, Jing Peiguang, Liu Yu. Learning-based stance-phase detection for a pedestrian dead-reckoning system with dynamic gait speeds[J]. Measurement Science and Technology,2021,32(10).

[2]]Li Wei, Chen Ruizhi, Yu Yue, Wu Yuan, Zhou Haitao. Pedestrian dead reckoning with novel heading estimation under magnetic interference and multiple smartphone postures[J]. Measurement,2021,182.

[3] Philip Handleman. DEAD RECKONING/OPERATION VENGEANCE [J]. Aviation History, 2021, 31(3).

[4] Daimler AG; Patent Issued for Noise Reflector For A Compressor Of A Turbomachine (USPTO 10,371,169)[J]. Journal of Engineering,2019.

[5] Robert LEHMENSIEK,Dirk I. L. DE VILLIERS. Noise Temperature Approximations for Offset Gregorian Reflector Systems[J]. IEICE Transactions on Communications, 2018, E101.B(2).

[6] M. M. Mikhailov,V. V. Sharafutdinova. Effect of electron energy on the accumulation of color centers in reflective coatings based on ZnO[J]. Russian Physics Journal, 1998, 41(4).